RAA 2015 Vol. **15** No. **12**, 2193–2203 doi: 10.1088/1674–4527/15/12/007
http://www.raa-journal.org *http://www.iop.org/journals/raa*

***R**esearch in*
***A**stronomy and*
***A**strophysics*

3D cluster members and near-infrared distance of open cluster NGC 6819

Xin-Hua Gao[1], Shou-Kun Xu[1] and Li Chen[2]

[1] School of Information Science and Engineering, Changzhou University, Changzhou 213164, China; *xhgcczu@163.com*
[2] Shanghai Astronomical Observatory, Chinese Academy of Sciences, Shanghai 200030, China; *chenli@shao.ac.cn*

Received 2015 March 19; accepted 2015 June 5

Abstract In order to obtain clean members of the open cluster NGC 6819, the proper motions and radial velocities of 1691 stars are used to construct a three-dimensional (3D) velocity space. Based on the DBSCAN clustering algorithm, 537 3D cluster members are obtained. From the 537 3D cluster members, the average radial velocity and absolute proper motion of the cluster are $V_{\rm r} = +2.30 \pm 0.04$ km s^{-1} and ($PM_{\rm RA}$, $PM_{\rm Dec}$) $= (-2.5 \pm 0.5, -4.3 \pm 0.5)$ mas yr^{-1}, respectively. The proper motions, radial velocities, spatial positions and color-magnitude diagram of the 537 3D members indicate that our membership determination is effective. Among the 537 3D cluster members, 15 red clump giants can be easily identified by eye and are used as reliable standard candles for the distance estimate of the cluster. The distance modulus of the cluster is determined to be $(m - M)_0 = 11.86 \pm 0.05$ mag (2355 ± 54 pc), which is quite consistent with published values. The uncertainty of our distance modulus is dominated by the intrinsic dispersion in the luminosities of red clump giants (~ 0.04 mag).

Key words: open clusters and associations: individual (NGC 6819) — Hertzsprung-Russell and C-M diagrams — stars: kinematics and dynamics — stars: distances

1 INTRODUCTION

Open clusters (OCs) have long been regarded as powerful tools for studies of stellar evolution and the Galactic disk (Friel 1995; Chen et al. 2003; Bonatto et al. 2006). Membership determination is the first important step for studies of OCs, which can directly influence the estimation of cluster astrophysical parameters. Various methods have been proposed for membership determination based on kinematic data, photometric data, positions and their combinations (Vasilevskis et al. 1958; Sanders 1971; Missana & Missana 1990; Cabrera-Cano & Alfaro 1990; Zhao & He 1990; Javakhishvili et al. 2006; Wu et al. 2006; Gao 2014). It is widely accepted that membership determinations based on the analysis of kinematic data (proper motions or radial velocities) are more reliable, because the mathematical models about stellar kinematics can be strictly established and membership probabilities can be easily obtained (Cabrera-Cano & Alfaro 1990). The stellar kinematic method applied to clusters (kinematic method), also known as the Vasilevskis-Sanders method, has been frequently used for the membership determination of OCs. However, the kinematic method strongly depends

on theoretical models of a stellar distribution, which are not always true (Cabrera-Cano & Alfaro 1990; Javakhishvili et al. 2006). Several methods have been proposed to conquer some of the problems arising from the kinematic method (Cabrera-Cano & Alfaro 1990; Javakhishvili et al. 2006; Wu et al. 2006; Gao 2014).

In our previous work, the DBSCAN clustering algorithm was used to segregate the members of OC NGC 188, where memberships are determined based only on 3D kinematics (Gao 2014). The DBSCAN clustering algorithm has the advantage of identifying arbitrarily shaped cluster structure and filtering noise well in high-dimensional space (Ester et al. 1996), which can be used to effectively segregate cluster members in 3D velocity space (proper motion and radial velocity) without any mathematical assumption about the stellar distribution (Gao 2014). With the rapid increase in highly-precise kinematic data, this method will continue to become more widely applied in this field.

In this paper, we attempt to obtain highly-accurate estimations of cluster members of OC NGC 6819 based on the DBSCAN clustering algorithm and highly-precise 3D kinematic data (proper motion and radial velocity). A certain number of red clump giants can be easily identified by eye from the color-magnitude diagram (CMD) of this cluster (Bragaglia et al. 2001; Anthony-Twarog et al. 2013, 2014; Lee-Brown et al. 2015). Red clump giants have been implemented as standard candles used for distance determination (Castellani et al. 1992; Paczyński & Stanek 1998; Stanek & Garnavich 1998; Udalski 2000; Alves 2000; Zhao et al. 2001; Pietrzyński et al. 2003; van Helshoecht & Groenewegen 2007; Groenewegen 2008; Gao & Chen 2012) and we will utilize these red clump giants to determine the distance to this cluster.

The data and method used in this work are described in Section 2. Section 3 presents the determination of the cluster distance. In Section 4, we compare our methods and results with those of other authors, and discuss differences between them.

2 DATA AND METHOD

2.1 Data

NGC 6819 ($l = 74.0°$, $b = +8.5°$) is a richly populated OC ($\sim$2.5 Gyr), the fundamental astrophysical parameters of which (e.g., age, distance, reddening and metallicity) have been investigated by many authors (Bragaglia et al. 2001; Lee-Brown et al. 2015; Rosvick & Vandenberg 1998; Kalirai et al. 2001; Kang & Ann 2002; Basu et al. 2011; Balona et al. 2013; Yang et al. 2013; Sandquist et al. 2013; Jeffries et al. 2013; Anthony-Twarog et al. 2014; Wu et al. 2014; Bedin et al. 2015). For the purpose of constructing 3D velocity space, we obtain a sample of 1691 stars with proper motions and radial velocities by cross-matching the two catalogs compiled by Platais et al. (2013) and Milliman et al. (2014). In order to eliminate any possible influence of binary stars from our results, the 1691 sample stars only include single stars confirmed by Milliman et al. (2014). The accuracy of proper motions for well-measured stars ranges from ~ 0.2 mas yr^{-1} within 10 arcmin of the cluster center to $\sim$ 1.1 mas yr^{-1} outside this radius (Platais et al. 2013). The accuracy of radial velocities of most sample stars is better than 1 km s^{-1} (Milliman et al. 2014). Highly-precise kinematic data mean high resolution in 3D velocity space, which is advantageous for membership determination of NGC 6819.

2.2 Method

The two input parameters of the DBSCAN clustering algorithm are set to (*Eps*, *MinPts*) $= (1, 30)$ after testing several times, which implies that if a point has more than 30 points in its *Eps*-neighborhood, including itself, it is a 'core' point (Ester et al. 1996). It is worth emphasizing that gravitationally bound OCs can reasonably be regarded as agglomerations of 'cold' stars immersed in the background of the 'hot' Galactic disk. This is because the typical velocity dispersion of Galactic OCs is on the order of 1 km s^{-1} or less but that of field-disk population stars is generally more

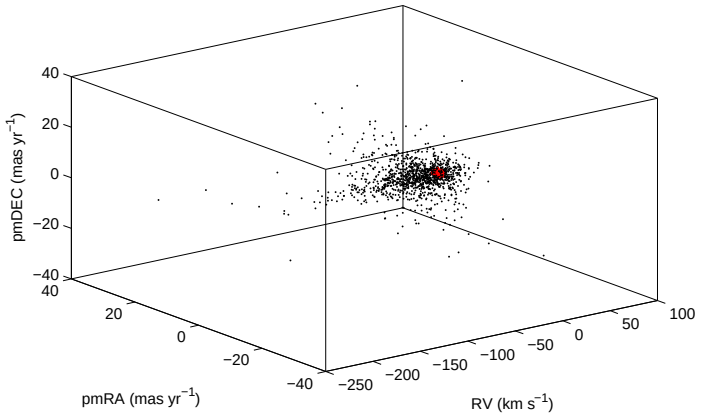

Fig. 1 Distribution of the 537 3D members (*red dots*) and field stars (*black dots*) in 3D velocity space.

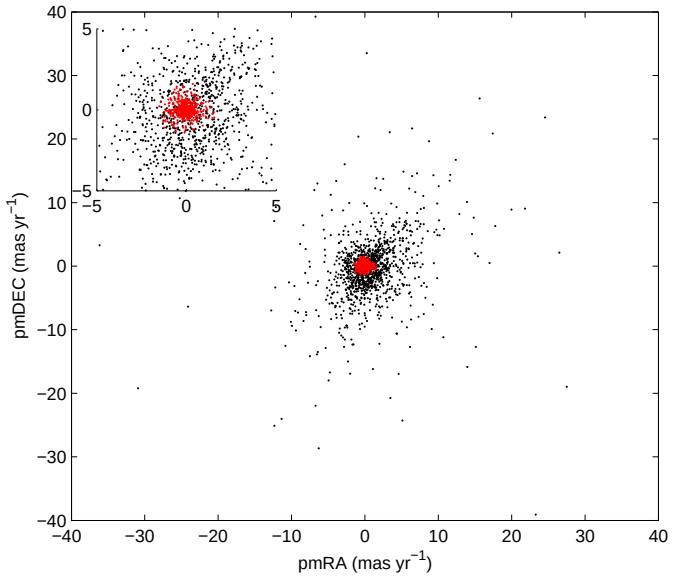

Fig. 2 Proper motion VPD of the 537 3D members (*red dots*) and field stars (*black dots*).

than 10∼20 times greater (Girard et al. 1989). In general, 'core' points contain a significantly larger number of points in their Eps-neighborhood than other types of points, so all 'core' points segregated by the DBSCAN algorithm can reasonably be considered as probable cluster members (Gao 2014). Here, it should be noted that the coverage of the 1691 radial velocities is much larger than that of the corresponding 1691 proper motions (Figs. 1–3), so all radial velocities are multiplied by a factor of 0.2 for the purpose of better clustering results (Gao 2014). Finally, 537 core points are obtained, all of which can be regarded as probable cluster members. Figure 1 shows the 3D distribution of the 537 3D members and field stars in the 3D velocity space.

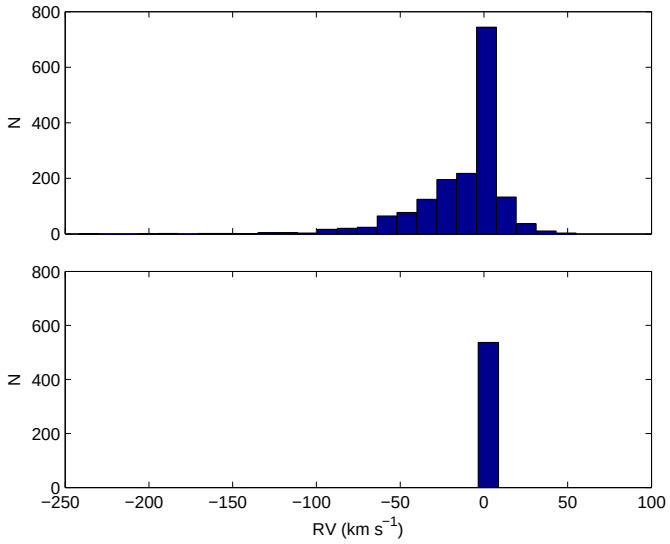

Fig. 3 Radial velocity histogram of the 1691 sample stars (*top panel*). Radial velocity histogram of the 537 3D members obtained from the DBSCAN clustering algorithm (*bottom panel*).

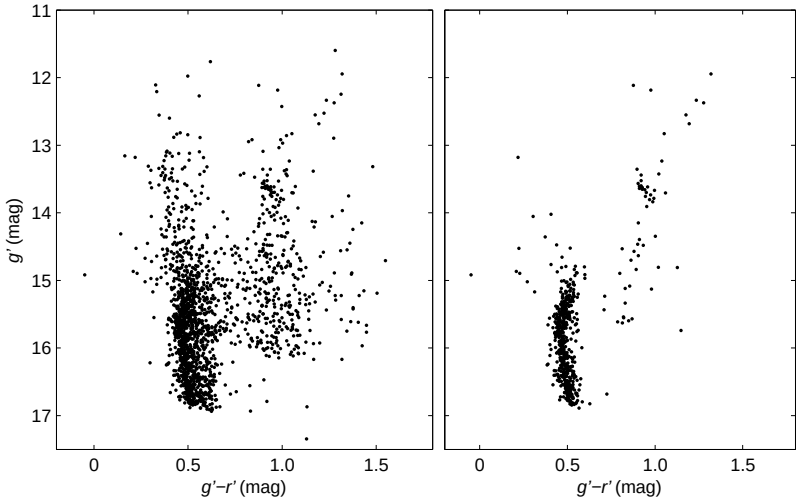

Fig. 4 CMD of the 1691 sample stars (*left panel*). CMD of the 537 3D members (*right panel*). The source of g' and r' photometric data is Platais et al. (2013).

As can be seen in Figure 2, the 537 3D members show a more compact shape than that of the field stars in the proper motion vector point diagram (VPD). Figure 3 shows that the 537 3D members share similar radial velocities. Figure 4 demonstrates that the CMD of the 537 3D members exhibits a well-defined main sequence and a red giant branch. Several blue stragglers can be easily identified in the CMD, which are located above and blueward of the turnoff point.

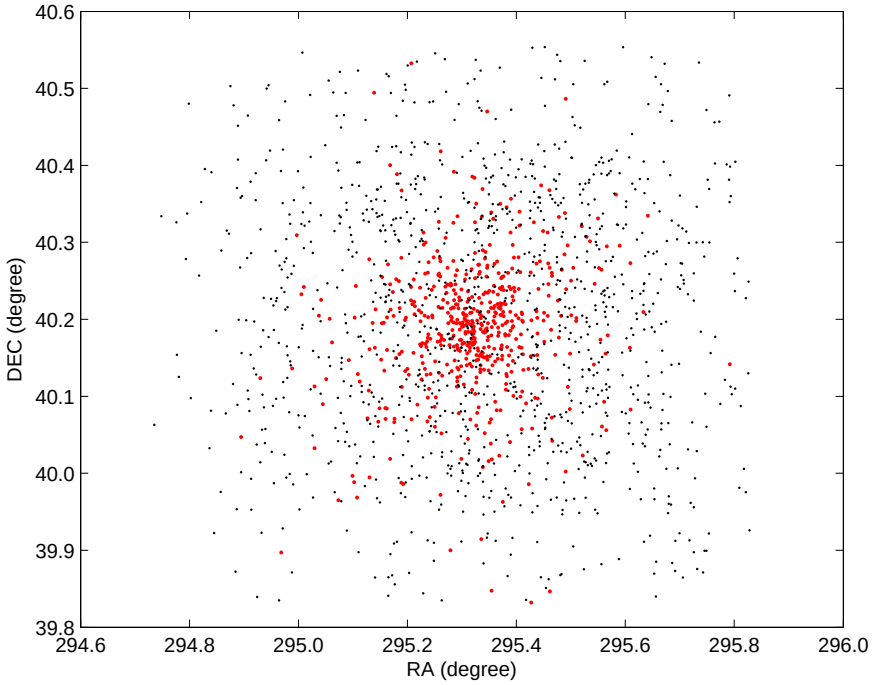

Fig. 5 Spatial distribution of the 537 3D cluster members (*red dots*) and field stars (*black dots*).

Figure 5 shows the spatial distribution of the 537 3D cluster members and field stars, in which cluster members are significantly more concentrated toward the cluster center compared with field stars. Among the 537 3D members, 514 stars (∼96%) have high membership probabilities (≥0.5) based on radial velocity (Milliman et al. 2014), while 495 stars (∼92%) have high membership probabilities (≥0.5) based on proper motion (Platais et al. 2013).

Figure 6 shows that quite a few likely field stars cannot be fully eliminated by simply using radial velocities (Milliman et al. 2014) or proper motions (Platais et al. 2013), but clean 3D members can be obtained by using the DBSCAN clustering algorithm and 3D kinematics. We can conclude that all of the 537 3D members derived from the DBSCAN clustering algorithm are likely cluster members.

To further confirm the effectiveness of our membership determination, we use the 537 3D members to calculate the weighted average radial velocity and its corresponding uncertainty based on the following equations:

$$V_{\rm r} = \frac{\sum(v_i \times w_i)}{\sum w_i}, \tag{1}$$

$$\sigma V_{\rm r} = \left[\frac{\sum((v_i - V_{\rm r})^2 \times w_i)}{(N-1) \times \sum w_i}\right]^{1/2}, \tag{2}$$

$$w_i = 1/(\sigma v_i)^2, \tag{3}$$

where $V_{\rm r}$ and $\sigma V_{\rm r}$ are the weighted average radial velocity and the corresponding uncertainty respectively, v_i is the radial velocity of the i-th 3D cluster member, w_i is the weight of the i-th 3D cluster member, σv_i is the observational error of the i-th 3D member, and N is the total number of 3D

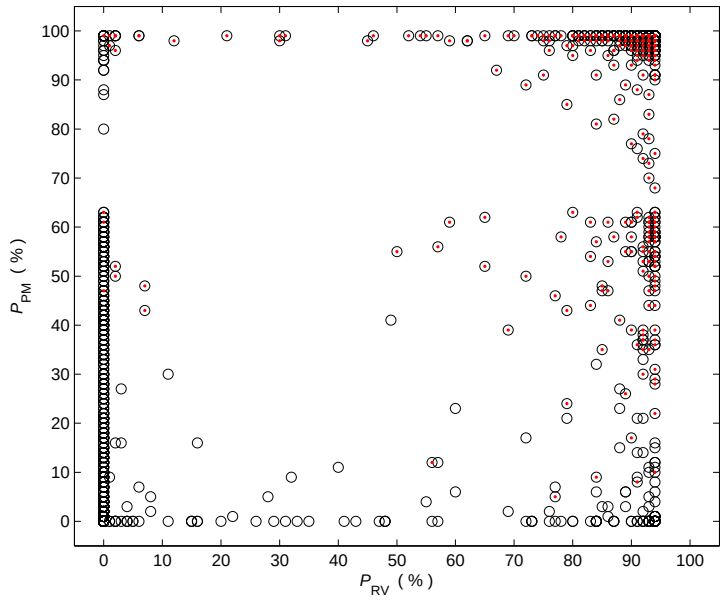

Fig. 6 The black circles indicate the radial-velocity membership probabilities ($P_{\rm RV}$) and proper motion membership probabilities ($P_{\rm PM}$) of the 1691 sample stars. The red dots indicate the radial-velocity membership probabilities and proper motion membership probabilities of our 537 3D members.

cluster members. Finally, the average radial velocity is determined to be $V_{\rm r} = +2.30 \pm 0.04$ km s^{-1}, which is quite consistent with the values derived by Milliman et al. (2014) and Hole et al. (2009). The average proper motion of the cluster is $(0.11 \pm 0.02, -0.12 \pm 0.02)$ mas yr^{-1}. It should be noted that four stars without observational proper motion error (0.00 mas yr^{-1}) were removed when the average proper motion was calculated. The total number of cluster members used for average proper motion determination is 533. After subtracting the average proper motion $(2.6 \pm 0.5, 4.2 \pm 0.5)$ mas yr^{-1} of ten external galaxies as described by Platais et al. (2013), the absolute proper motion of the cluster is ($PM_{\rm RA}$, $PM_{\rm Dec}$) $= (-2.5 \pm 0.5, -4.3 \pm 0.5)$ mas yr^{-1}, and this value is quite consistent with the value derived by Platais et al. (2013). So, we can safely say that the 537 3D members obtained based on the DBSCAN clustering algorithm represent a rather pure sample of members of this cluster.

In Table 1, we list equatorial position (RA, Dec), radial velocity and observational error (RV, eRV), proper motion (pmRA, pmDEC) and observational error (epmRA, epmDEC), magnitude (g') and color ($g' - r'$) for the 537 3D members. This table is presented in its entirety in the electronic version of this article (*http://www.raa-journal.org/docs/Supp/2208Table1.txt*) and a portion is shown here for guidance regarding the form and content.

3 NEAR-INFRARED DISTANCE

The determination of accurate distances plays a key role in studying any OC. The distance of NGC 6819 has been thoroughly-investigated by many authors (Rosvick & Vandenberg 1998, Kalirai et al. 2001; Kang & Ann 2002; Basu et al. 2011; Balona et al. 2013; Yang et al. 2013; Sandquist et al. 2013; Jeffries et al. 2013; Anthony-Twarog et al. 2014; Wu et al. 2014; Bedin et al. 2015). Among our 537 3D members, several red clump giants can be easily identified by eye from their

Table 1 Fundamental Parameters Describing the 537 3D Members

RA (°)	Dec (°)	RV (km s^{-1})	eRV (km s^{-1})	pmRA (mas yr^{-1})	epmRA (mas yr^{-1})	pmDEC (mas yr^{-1})	epmDEC (mas yr^{-1})	g' (mag)	$g'-r'$ (mag)
295.28529	+40.39158	1.49	0.58	–0.12	0.24	–0.37	0.60	16.299	0.456
295.58304	+40.36206	2.96	0.40	0.73	1.70	0.70	0.22	16.202	0.529
295.60858	+40.16289	1.19	0.26	–0.21	0.83	1.48	0.67	16.811	0.523
295.30329	+40.20664	2.91	0.10	0.00	0.22	0.40	0.12	13.628	0.917
295.42725	+39.83200	3.26	0.75	–1.24	0.70	–1.10	0.70	16.600	0.525
...	...	...	...	...	...	...	...	...	...

Table 2 Fundamental Parameters Describing the 15 Red Clump Giants

ID	RA (°)	Dec (°)	J (mag)	eJ (mag)	$K_{\rm s}$ (mag)	$eK_{\rm s}$ (mag)
01	295.37308	+40.20583	10.922	0.021	10.207	0.013
02	295.33950	+40.23258	10.939	0.020	10.250	0.018
03	295.37258	+40.23889	10.990	0.021	10.263	0.011
04	295.30646	+40.20572	10.969	0.023	10.268	0.018
05	295.37146	+40.21781	10.973	0.020	10.305	0.018
06	295.30329	+40.20664	10.991	0.024	10.311	0.022
07	295.28579	+40.22497	10.990	0.021	10.312	0.018
08	295.34262	+40.27894	11.024	0.020	10.312	0.017
09	295.39350	+40.14614	11.005	0.021	10.323	0.011
10	295.30604	+40.19894	10.992	0.020	10.323	0.018
11	295.27183	+40.23450	11.026	0.020	10.337	0.018
12	295.28858	+40.24544	11.005	0.020	10.341	0.018
13	295.20917	+40.21972	11.009	0.020	10.346	0.018
14	295.31517	+40.16961	11.062	0.020	10.358	0.018
15	295.30100	+40.19275	11.079	0.026	10.358	0.023

positions in the CMD (see Fig. 4). The absolute magnitudes of red clump giants have been demonstrated to be weakly correlated with their chemical abundances and ages, which makes red clump giants reliable standard candles used in distance determination (Castellani et al. 1992; Paczyński & Stanek 1998; Stanek & Garnavich 1998; Udalski 2000; Alves 2000; Zhao et al. 2001; Pietrzyński et al. 2003; van Helshoecht & Groenewegen 2007; Groenewegen 2008; Gao & Chen 2012). 2MASS photometric data (Skrutskie et al. 2006) are very suitable for segregating red clump giants (López-Corredoira et al. 2014). Moreover, the near-infrared absolute magnitudes of red clump giants only vary a little with their chemical abundances and ages (Alves 2000; Pietrzyński et al. 2003; van Helshoecht & Groenewegen 2007; Groenewegen 2008), and the K-band absolute magnitudes of red clump giants have been thoroughly-investigated (Alves 2000; van Helshoecht & Groenewegen 2007; Groenewegen 2008). Among our 537 3D cluster members, 496 stars have high-quality 2MASS photometric data, and 15 red clump giants can be easily identified in the 2MASS CMD (see Fig. 7). The fundamental parameters describing the 15 red clump giants are listed in Table 2.

The average $K_{\rm s}$-band magnitude of the 15 red clump giants can be determined using the following equations:

$$mK_{\rm s} = \frac{\sum(K_{\rm si} \times w_i)}{\sum w_i}, \tag{4}$$

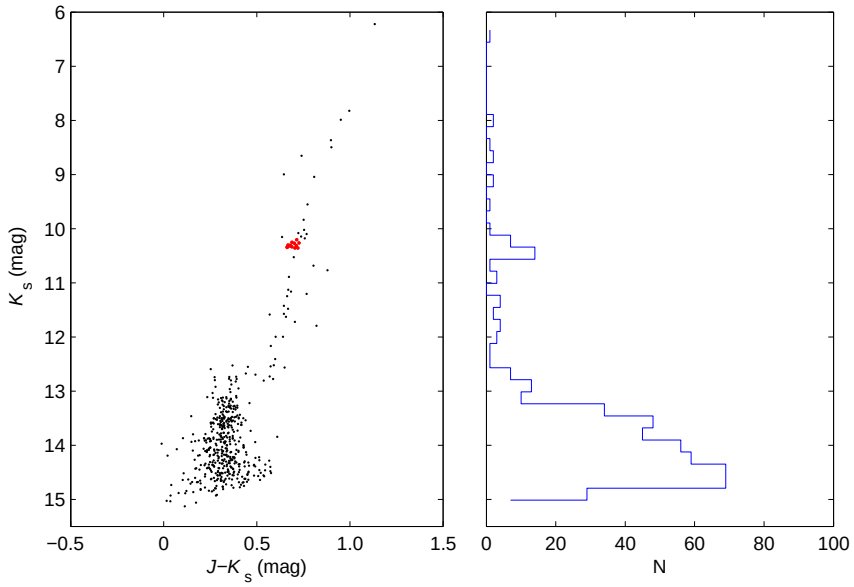

Fig. 7 2MASS CMD (J-K_s vs. K_s) of 496 3D cluster members (*left panel*). The red dots indicate the 15 red clump giants. K_s-band magnitude distribution of 496 3D cluster members (*right panel*).

$$\sigma mK_\mathrm{s} = \left[\frac{\sum(K_\mathrm{si} - mK_\mathrm{s})^2}{(N-1)}\right]^{1/2}, \quad (5)$$

$$w_i = 1/(eK_\mathrm{si})^2, \quad (6)$$

where mK_s and σmK_s are the average K_s-band 2MASS magnitude and the corresponding uncertainty respectively, K_si is the K_s-band magnitude of i-th red clump giant, eK_si is the observational error of the i-th red clump giant, N is the total number of red clump giants, and w_i is the weight of the i-th red clump giant. Finally, the average K_s-band magnitude is determined to be $mK_\mathrm{s} = 10.299 \pm 0.044$ mag. The distance modulus and the corresponding distance of the cluster can be determined based on the following equations:

$$(m-M)_0 = mK_\mathrm{s} - MK_\mathrm{s} - AK_\mathrm{s}, \quad (7)$$

$$AK_\mathrm{s} = 3.1 \times E(B-V) \times (AK_\mathrm{s}/AV), \quad (8)$$

$$D = 10^{[\frac{(m-M)_0}{5}+1]}, \quad (9)$$

where $(m-M)_0$ is the distance modulus of the cluster, mK_s is the average K_s-band magnitude of the 15 red clump giants, MK_s is the absolute Ks-band magnitude of the 15 red clump giants, AK_s is K_s-band interstellar extinction, $E(B-V)$ is interstellar reddening, AV is V-band interstellar extinction, and D is distance (unit: pc). By adopting $mK_\mathrm{s} = 10.299 \pm 0.044$ mag, $MK_\mathrm{s} = -1.61 \pm 0.03$ mag (Alves 2000), $E(B-V) = 0.14$ mag (Bragaglia et al. 2001) and $AK_\mathrm{s}/AV = 0.12$ (Dutra et al. 2002), the near-infrared distance modulus $(m-M)_0 = 11.86 \pm 0.05$ mag ($D = 2355 \pm 54$ pc) is obtained and the relative error of the distance is ∼2.3%.

Table 3 Listing of the Distance Moduli of NGC 6819

$(m-M)_0$ (mag)	$E(B-V)$ (mag)	Method	Reference
11.76	0.28	main sequence stars	Auner 1974
11.85[a]	0.16	isochrone	Rosvick & Vandenberg 1998
11.99±0.18	0.10	isochrone	Kalirai et al. 2001
11.8	0.10	isochrone	Kang & Ann 2002
11.85±0.05	0.15	asteroseismology	Basu et al. 2011
11.88±0.08	0.15	asteroseismology	Balona et al. 2013
11.94±0.04	0.15	isochrone	Balona et al. 2013
11.74±0.06[a]	0.15	red giants	Balona et al. 2013
11.93±0.10	0.14	isochrone	Yang et al. 2013
12.02±0.09[a]	0.12	binary star	Sandquist et al. 2013
12.00±0.05	0.12	dwarf stars	Jeffries et al. 2013
12.07[a]	0.14	isochrone	Anthony-Twarog et al. 2013
11.90±0.12[a]	0.16	isochrone	Anthony-Twarog et al. 2014
12.00±0.06	0.13	isochrone	Wu et al. 2014
11.83±0.14	0.14	asteroseismology	Wu et al. 2014
11.88±0.14	0.14	asteroseismology	Wu et al. 2014
11.88±0.11	0.17	isochrone	Bedin et al. 2015
11.86±0.05	0.14	red clump giants	this work

Notes: Superscript a indicates that this value is determined from the formula: $(m-M)_0 = (m-M)_V - 3.1 \times E(B-V)$.

The intrinsic dispersion of the $K_{\rm s}$ magnitudes, $\sigma_0 K_{\rm s}$, for the 15 red clump giants can be estimated using the following formula

$$\sigma_0 K_{\rm s} = \left[\frac{\sum (K_{\rm si} - mK_{\rm s})^2}{(N-1)} - \frac{\sum eK_{\rm si}^2}{N}\right]^{1/2}, \quad (10)$$

where $K_{\rm si}$ is the $K_{\rm s}$-band magnitude of the i-th red clump giant, $mK_{\rm s}$ is the average $K_{\rm s}$-band magnitude of the 15 red clump giants, $eK_{\rm si}$ is the observational error of the i-th red clump giant, and N is the total number of red clump giants. The intrinsic dispersion $\sigma_0 K_{\rm s}$ (~ 0.04 mag) indicates that the uncertainty of our distance modulus is dominated by the intrinsic dispersion in the $K_{\rm s}$ magnitudes of the red clump giants. This is not surprising since the average photometric error of the $K_{\rm s}$ magnitudes for the 15 red clump giants is ~ 0.017 mag (see Table 2). Our distance modulus based on the 15 red clump giants is quite consistent with most of the values derived based on other methods and data (see Table 3).

Previous works have shown that NGC 6819 suffers from differential reddening (Platais et al. 2013; Anthony-Twarog et al. 2014). The maximum of the differential reddening across the cluster reaches $\Delta E(B-V) = 0.06$ mag (Platais et al. 2013; Anthony-Twarog et al. 2014), which may affect the distance determination by isochrone fitting (Yang et al. 2013; Bonatto et al. 2006; An et al. 2007) or asteroseismology (Wu et al. 2014). Yang et al. (2013) pointed out that a change in $E(B-V)$ of ± 0.04 mag may yield an error in the distance modulus of ± 0.05 mag, and a change in the chemical abundance of ± 0.1 dex may result in a change in the distance modulus of ± 0.08 mag when using isochrone fitting. Wu et al. (2014) indicate that a change of 0.01 mag in $E(B-V)$ may lead to an uncertainty of at least 0.04 mag in distance modulus when using asteroseismology. As we mentioned earlier, because the $K_{\rm s}$-band extinction is much smaller than that of the optical band ($AK_{\rm S}/AV = 0.12$), our distance modulus is almost not affected by the differential reddening across the cluster. The $K_{\rm s}$-band absolute magnitudes of red clump giants are weakly correlated with their chemical abundances and ages. So, our distance modulus is almost independent of the chemical abundance and age of the cluster.

4 CONCLUSIONS AND DISCUSSION

In this paper, we employed the DBSCAN clustering algorithm and highly-precise 3D kinematic data of 1691 single stars to obtain 537 3D cluster members of OC NGC 6819. The average proper motion and radial velocity of the cluster are not significantly different from those of surrounding field stars (Figs 1–3), which makes it hard to obtain clean cluster members from surrounding field stars with the traditional kinematic method (Cabrera-Cano & Alfaro 1990; Gao & Chen 2010). Our 537 3D members are most probably cluster members according to their proper motions, radial velocities, spatial distribution and morphology of the CMD. Moreover, our method can obtain reliable cluster members in appropriate high-dimensional space without any mathematical models. Unlike the traditional kinematic method (Zhao & He 1990), the DBSCAN clustering algorithm does not rely on strict mathematical models, so it cannot provide analytic membership probabilities for cluster members. Therefore, it is hard to quantitatively describe effects of the accuracy associated with the radial velocities and proper motions. Fortunately, most of the 1691 sample stars have sufficiently accurate radial velocities and proper motions.

Using the 15 red clump giants selected from the 537 3D cluster members, we determined the distance modulus based on near-infrared data of the cluster. Our value is quite consistent with most of the published values obtained using other methods and data (Basu et al. 2011; Balona et al. 2013; Yang et al. 2013; Wu et al. 2014; Bedin et al. 2015). The major advantage of our method is that red clump giants have almost the same near-infrared luminosity and the luminosity is almost not affected by their differential reddening, chemical abundances or ages. The effects of the differential reddening, chemical abundance and age of the cluster were ignored when the distance modulus was determined, but the derived value seems to be reliable.

Acknowledgements This research was supported by the National Natural Science Foundation of China (NSFC, Grant No. 11403004) and the School Foundation of Changzhou University (ZMF 1002121). C.L. would like to acknowledge support by the 973 Program (2014 CB845702), the Strategic Priority Research Program “The Emergence of Cosmological Structures” of the Chinese Academy of Sciences (CAS; grant XDB09010100) and by the NSFC (Grant No. 11373054). The authors are grateful for the insightful comments of an anonymous referee, which greatly improved the article. This research has made use of the VizieR catalogue access tool, CDS, Strasbourg, France.

References

Alves, D. R. 2000, ApJ, 539, 732
An, D., Terndrup, D. M., Pinsonneault, M. H., et al. 2007, ApJ, 655, 233
Anthony-Twarog, B. J., Deliyannis, C. P., Rich, E., & Twarog, B. A. 2013, ApJ, 767, L19
Anthony-Twarog, B. J., Deliyannis, C. P., & Twarog, B. A. 2014, AJ, 148, 51
Auner, G. 1974, A&AS, 13, 143
Balona, L. A., Medupe, T., Abedigamba, O. P., et al. 2013, MNRAS, 430, 3472
Basu, S., Grundahl, F., Stello, D., et al. 2011, ApJ, 729, L10
Bedin, L. R., Salaris, M., Anderson, J., et al. 2015, MNRAS, 448, 1779
Bonatto, C., Kerber, L. O., Bica, E., & Santiago, B. X. 2006, A&A, 446, 121
Bragaglia, A., Carretta, E., Gratton, R. G., et al. 2001, AJ, 121, 327
Cabrera-Cano, J., & Alfaro, E. J. 1990, A&A, 235, 94
Castellani, V., Chieffi, A., & Straniero, O. 1992, ApJS, 78, 517
Chen, L., Hou, J. L., & Wang, J. J. 2003, AJ, 125, 1397
Dutra, C. M., Santiago, B. X., & Bica, E. 2002, A&A, 381, 219
Ester, M., Kriegel, H.-P., Sander, J., & Xu, X. 1996, in KDD Proceedings, 96, 226
Friel, E. D. 1995, ARA&A, 33, 381

Gao, X.-H., & Chen, L. 2010, RAA (Research in Astronomy and Astrophysics), 10, 761
Gao, X.-H., & Chen, L. 2012, Chinese Astronomy and Astrophysics, 36, 1
Gao, X.-H. 2014, RAA (Research in Astronomy and Astrophysics), 14, 159
Girard, T. M., Grundy, W. M., Lopez, C. E., & van Altena, W. F. 1989, AJ, 98, 227
Groenewegen, M. A. T. 2008, A&A, 488, 935
Hole, K. T., Geller, A. M., Mathieu, R. D., et al. 2009, AJ, 138, 159
Javakhishvili, G., Kukhianidze, V., Todua, M., & Inasaridze, R. 2006, A&A, 447, 915
Jeffries, Jr., M. W., Sandquist, E. L., Mathieu, R. D., et al. 2013, AJ, 146, 58
Kalirai, J. S., Richer, H. B., Fahlman, G. G., et al. 2001, AJ, 122, 266
Kang, Y.-W., & Ann, H. B. 2002, Journal of Korean Astronomical Society, 35, 87
Lee-Brown, D. B., Anthony-Twarog, B. J., Deliyannis, C. P., Rich, E., & Twarog, B. A. 2015, AJ, 149, 121
López-Corredoira, M., Abedi, H., Garzón, F., & Figueras, F. 2014, A&A, 572, A101
Milliman, K. E., Mathieu, R. D., Geller, A. M., et al. 2014, AJ, 148, 38
Missana, M., & Missana, N. 1990, AJ, 100, 1850
Paczyński, B., & Stanek, K. Z. 1998, ApJ, 494, L219
Pietrzyński, G., Gieren, W., & Udalski, A. 2003, AJ, 125, 2494
Platais, I., Gosnell, N. M., Meibom, S., et al. 2013, AJ, 146, 43
Rosvick, J. M., & Vandenberg, D. A. 1998, AJ, 115, 1516
Sanders, W. L. 1971, A&A, 14, 226
Sandquist, E. L., Mathieu, R. D., Brogaard, K., et al. 2013, ApJ, 762, 58
Skrutskie, M. F., Cutri, R. M., Stiening, R., et al. 2006, AJ, 131, 1163
Stanek, K. Z., & Garnavich, P. M. 1998, ApJ, 503, L131
Udalski, A. 2000, ApJ, 531, L25
van Helshoecht, V., & Groenewegen, M. A. T. 2007, A&A, 463, 559
Vasilevskis, S., Klemola, A., & Preston, G. 1958, AJ, 63, 387
Wu, T., Li, Y., & Hekker, S. 2014, ApJ, 786, 10
Wu, Z.-Y., Zhou, X., Ma, J., Jiang, Z.-J., & Chen, J.-S. 2006, PASP, 118, 1104
Yang, S.-C., Sarajedini, A., Deliyannis, C. P., et al. 2013, ApJ, 762, 3
Zhao, G., Qiu, H. M., & Mao, S. 2001, ApJ, 551, L85
Zhao, J. L., & He, Y. P. 1990, A&A, 237, 54